Quantum and classical vibrational chaos in floppy molecules

Stavros C. Farantos[a)]
Theoretical and Physical Chemistry Institute, National Hellenic Research Foundation, 48 Vas. Constantinou Avenue, Athens 116/35, Greece

Jonathan Tennyson
Science and Engineering Research Council, Daresbury Laboratory, Daresbury, Warrington WA4 4AD, England

(Received 23 July 1984; accepted 10 October 1984)

Classical and quantum mechanical calculations on the vibrational motions of LiCN using a realistic potential are presented. These, together with recent results for KCN, are analyzed using indicators that have been proposed for identifying quantum chaos. These are nodal structure, dominant coefficient, overlapping avoided crossings, second differences, and spectral distribution. We find an early onset of chaos in LiCN and KCN with good agreement between the indicators. Localized quasiperiodic trajectories and regular states are found well into the chaotic region for both isomers of LiCN. LiCN is a weakly coupled system in contrast to strongly coupled KCN. The utility of the indicators is discussed in the light of these results. The link between floppy molecules and chaos suggests that floppy systems are suitable for the experimental investigation of vibrational chaos.

I. INTRODUCTION

Many systems when studied using classical mechanics show transitions from a low energy regime with regular (quasiperiodic) trajectories to a higher energy regime which has an increasing proportion of irregular (chaotic) trajectories. The properties of such systems have been well studied and a good understanding of classical chaos has been achieved.[1] In particular the power spectrum of a trajectory, its Poincaré surfaces of section and plots of the trajectory itself, as well as the maximal Lyapunov number,[2–4] give criteria which enable chaotic regions to be identified.

Quantum mechanically the situation is less clear. Much work has been done on model problems,[5–20] such as the Hénon–Heiles Hamiltonian, trying to identify a quantum analog to classical chaos. Although several indicators have been proposed, at this time the exact nature of quantum chaos is still a subject of controversy. No true signature of chaos has yet emerged.

The occurrence of classical chaos is often used as an indicator for quantum chaos, indeed it would be unwise to search for quantum chaos without first testing the classical properties of a system. Although it is now widely accepted that there is no one-to-one correspondence between classical and quantum chaos,[20,21] we know of no case where quantum chaos has been postulated for a classically quasiperiodic regime.[22] Indeed, the explanation that the "sluggish" onset of quantum chaos relative to classical chaos is due to the finite value of $\hbar$[6,23] would appear to imply that classical chaos is a necessary but not sufficient condition for quantum chaos. Contrary to this Reinhardt has stated that "*quantum chaos and classical chaos do not imply each other.*"[21]

Among the means that have been suggested for identifying quantum chaos, five are sufficiently general to be applied to quantum mechanical calculations on real systems. These are the criteria of nodal structure,[7] dominant coefficients,[8] second differences,[9] overlapping avoided crossings,[10,23] and spectral distribution.[11,24]

For regular states the nodes of a multidimensional wave function form a grid which allows quantum numbers for each coordinate to be assigned by inspection. This regular structure can be associated with an approximate separability of coordinates and hence integrability. As was first observed semiclassically,[7] some high energy states lose this nodal regularity so that quantization along qualitatively separable coordinates can no longer be achieved. It has been suggested that these irregular states are quantum chaotic, although recent work by De Leon *et al.*[12] has shown that regular states in resonance can also have nodal structures which appear irregular.

A related quantitative method of assigning regular or quasiperiodic states has been proposed by Hose and Taylor.[8] They show that any state which has a coefficient greater than $(0.5)^{1/2}$ in a basis function expansion can be assigned as regular with the quantum numbers of the dominant basis function. Furthermore, they use this feature as the basis of a quantum KAM theory. However, this indicator is of limited usefulness as it depends on a fortunate choice of basis and says nothing about states which fail to satisfy it.

Two related measures of quantum chaos have been suggested, based on Percival's conjecture[25] that irregular states will be highly sensitive to perturbations. Pomphrey[9] analyzed energy levels of the Hénon–Heiles Hamiltonian and classified states as regular or chaotic according to the

[a)] Permanent address: Department of Chemistry, University of Crete, Iraklion, P.O. Box 1470, Crete, Greece.

 0021-9606/85/020800-10$02.10 © 1985 American Institute of Physics

Downloaded 08 Dec 2008 to 194.177.215.121. Redistribution subject to AIP license or copyright; see http://jcp.aip.org/jcp/copyright.jsp

magnitude of energy second difference with respect to small changes in the coupling potential. This measure has since been questioned[13,14] but supported by Edmonds *et al.*[6]

Another manifestation of this instability, a dense web of overlapping avoided crossings, has been noted by Marcus and co-workers.[10,23] This criterion for quantum chaos has since been applied to several systems.[11,13,15]

Analysis of the nearest neighbor spacings of energy levels has led to the identification of different distributions for quasiperiodic and chaotic regions of the spectrum. Berry and Tabor[16] have shown semiclassically that regular levels should follow a Poisson distribution. Numerical experiments with random matrices have led to the suggestion that chaotic spectra should obey a Dyson–Wigner distribution.[24,26] This criterion has special appeal as it can be applied to experimental data (see, e.g., Refs. 26 and 27).

A limiting form for the chaotic distribution for the case where the energy level spacing tends to zero has been suggested by Berry,[28] which agrees with the Dyson–Wigner distribution.

The indicators discussed above are not the only ones that have been suggested. Time-dependent problems have been analyzed using wave packets,[5,14,17] correlation functions,[5,18,19] overlaps[29] and Wigner phase-space distributions.[17] We are interested in time-independent solutions of real systems and will not consider any of these further.

The ultimate aim of studying quantum chaos must be the understanding of its experimental manifestation. However, as work on HCN has shown,[30] this cannot easily be achieved by the direct comparison of classical calculation with experiment. This is because the vibrational motion of a system, despite being completely determined by the potential energy surface of that system, is unstable in chaotic regions to small changes to this potential. Therefore we believe that the correct approach is through the study of real systems which display classical chaos, quantum mechanically. In this way we hope to gain understanding of when and how quantum chaos might manifest itself and perhaps suggest how such chaos might be observed. Furthermore, the scarcity of nonlinear mechanical analysis of real potentials underlines the need for systematic studies of realistic potentials.[2,30]

Floppy molecules have excited much recent interest among experimentalists[31–33] and quantum theorists.[34–38] The large amplitude vibrations of these molecules sample large regions of the potential and can thus be expected to be significantly anharmonic. Classical calculations have shown that the onset of chaos in a system is closely related to the anharmonicity of that system. Floppy molecules would thus appear excellent candidates for the early onset of chaos. Indeed, if one was to apply the criterion of nodal structure to some published results,[35,37] this chaos has already been found, but passed unnoticed.

In a recent paper,[39] henceforth referred to as I, we gave preliminary results for the floppy KCN system. Classically, vibrational chaos was found at very low energies, even below the quantum ground state of the system. Use of the indicators discussed above enabled us to establish the early onset of quantum chaos although some quantum sluggishness was observed.

In this paper we present results on the vibrations of LiCN, computed using both quantum and classical mechanics. Although both KCN and LiCN are floppy, they can be expected to show very different behavior. KCN has a triangular minimum energy structure and a low-lying barrier at the linear KNC geometry.[40] Conversely, the LiCN potential we use has an absolute minimum for linear LiNC and a local minimum for linear LiCN. This potential, calculated *ab initio* by Essers *et al.*,[41] predicts an equilibrium structure in good agreement with recent microwave results.[33] Calculations using this potential[36] gave fundamental vibrations near those observed in matrix isolation studies,[42] they also predicted that both minima support localized vibrational states and that many of the higher states are delocalized.

In this work, as in previous theoretical studies on LiCN and KCN[35–42] only the two-dimensional vibrational problem given by freezing the CN bond, will be considered. This approximation is physically motivated because of the weak coupling between M^+ and CN^- coordinates[40] and the high frequency of the CN^- fundamental vibration. We thus consider only a two-dimensional vibrational problem and leave the full problem for future study.

By analyzing the vibrational motion of LiCN and KCN, we hope to assess the performance of the five indicators for quantum chaos on real systems and their usefulness in the search for chaos in multidimensional systems with real potentials. We also seek to establish the link between floppy molecules and low lying vibrational chaos.

II. CLASSICAL CALCULATIONS ON LiCN

Like that used for KCN, the LiCN potential of Esser *et al.*[41] is expressed analytically as a Legendre expansion in scattering coordinates

$$V(R, \theta) = \sum_{\lambda=0}^{9} P_\lambda(\cos\theta) V_\lambda(R), \tag{1}$$

where R is the distance from Li^+ to the CN^- center-of-mass and θ is the angle between R and the CN^- bond, which has length r. θ is measured from the linear LiCN structure and r frozen at $2.186a_0$.

The Hamiltonian for this rotationless two dimensional vibrational problem is

$$H = \frac{P_R^2}{2\mu_1} + \left(\frac{1}{2\mu_1 R^2} + \frac{1}{2\mu_2 r^2}\right) P_\theta^2 + V(R, \theta), \tag{2}$$

where

$$\mu_1^{-1} = m_{\mathrm{Li}}^{-1} + (m_{\mathrm{C}} + m_{\mathrm{N}})^{-1},$$

$$\mu_2^{-1} = m_{\mathrm{C}}^{-1} + m_{\mathrm{N}}^{-1}. \tag{3}$$

m_{Li}, m_{C}, and m_{N} denote atomic masses.

The four first order Hamilton's equations were integrated by an Adams–Moulton fifth order predictor sixth order corrector method initialized with a fourth

Downloaded 08 Dec 2008 to 194.177.215.121. Redistribution subject to AIP license or copyright; see http://jcp.aip.org/jcp/copyright.jsp

order Runge–Kutta procedure. The trajectories were integrated for about 1 ps and the energy was conserved to seven figures.

In classical mechanics there are four methods of deciding whether a trajectory is quasiperiodic or chaotic.[1] These are (a) the study of power spectrum of a dynamical variable, (b) the Poincaré surfaces of section, (c) inspection of the projection of the trajectory onto a coordinate plane and (d) the calculation of the rate of exponential divergence of two neighboring trajectories.

To have a view of the global structure of phase space in quasiperiodic-chaotic regions at different energies, we first examined trajectories the initial conditions of which were chosen randomly over phase space. We used an orthant sampling method[43] to generate random unit four vectors in phase space and then scaled them appropriately to conserve energy. LiCN shows a typical KAM behavior.[44] At energies below 1600 cm^{-1} the phase space is occupied mostly by quasiperiodic trajectories. At higher energies chaotic trajectories coexist with quasiperiodic ones and their measure increases with energy. By using batches of 50 pairs of trajectories we have calculated average values of the maximal Lyapunov number for the chaotic trajectories (Fig. 1). These values were obtained by evaluating the rate of exponential divergence of 2^{11} time steps. It has been shown[45] that this stochastic parameter is proportional to what is called the Kolmogorov entropy. It has been conjectured[46] that the inverse of the Kolmogorov entropy gives the time scale for energy randomization in the system. This conjecture has been supported by tests on model[47] and real systems.[2–4] From Fig. 1 we can see that, as for KCN, chaos starts early if we compare the critical energy to transition with the dissociation energy (53 684.688 cm^{-1} = 6.656 eV).

Next we examined individual trajectories started at the equilibrium geometry of both LiNC and LiCN. The energy was initially distributed as kinetic energy in the bending and stretching modes. Figure 2 shows typical

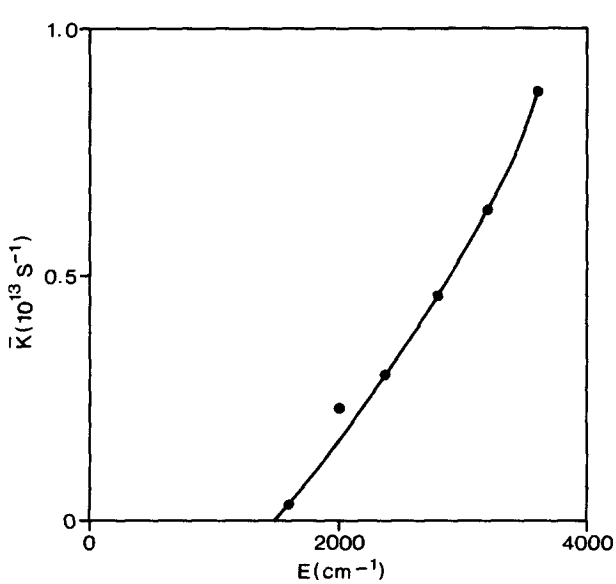

FIG. 1. Average values for the rate of divergence of two neighboring trajectories for LiNC.

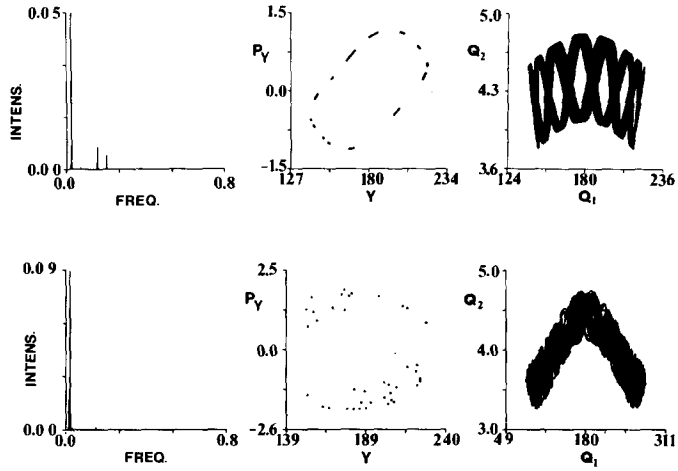

FIG. 2. Typical quasiperiodic and chaotic trajectories for LiNC below the isomerization barrier. E = 2456 cm^{-1} (upper) and 2341 cm^{-1} (lower). (a) The power spectrum in eV (1 eV = 8065 cm^{-1}), (b) Poincaré surface of section, and (c) projection of the trajectory on the coordinate plane. Q_1 is θ in degrees and Q_2 is R in a_0.

LiNC quasiperiodic and chaotic trajectories. Both trajectories lie below the barrier to isomerization (3377 cm^{-1}). Similarly Fig. 3 shows a trajectory for LiCN, for which the energy is given relative to the LiCN minimum, which is 2281 cm^{-1} above the LiNC absolute minimum.

We found quasiperiodic trajectories above the barrier to isomerization for both LiNC and LiCN. Figure 4 shows two such trajectories. However, chaotic trajectories above the barrier are no longer localized around LiNC or LiCN, but jump from one minimum to the other. As can be seen in Fig. 5 the angle θ increases beyond 360° demonstrating the rotation of Li^+ around CN^-.

In the next sections we show that the types of trajectories distinguished above have analogous quantum states.

III. QUANTUM CALCULATIONS ON LiCN

Only the vibrational levels of LiCN with zero total angular momentum, $J = 0$, will be considered. Following Tennyson and Sutcliffe,[36] the Hamiltonian can be written

$$H = -\frac{\hbar^2}{2\mu_1 R^2}\frac{\partial}{\partial R}\left(R^2\frac{\partial}{\partial R}\right) - \frac{\hbar^2}{2}\left(\frac{1}{\mu_1 R^2} + \frac{1}{\mu_2 r^2}\right) \times \frac{1}{\sin\theta}\frac{\partial}{\partial\theta}\left(\sin\theta\frac{\partial}{\partial\theta}\right) + V(R,\theta) \quad (4)$$

which is the quantum analog of Eq. (2). A convenient method of solving Eq. (4) is via a basis set expansion. Use of Legendre functions for the angular coordinates allows integrals in this coordinate to be performed analytically.

In this work we make two changes from calculations on LiCN by Brocks and Tennyson.[37] Firstly, for consistency with the results obtained for KCN, we use a CN bondlength of $r = 2.186a_0$. Secondly, for the radial coordinate basis we choose the Morse oscillator-like functions of Tennyson and Sutcliffe,[36] rather than the numerical functions which Brocks and Tennyson[37] found rather unsatisfactory for this problem.

Downloaded 08 Dec 2008 to 194.177.215.121. Redistribution subject to AIP license or copyright; see http://jcp.aip.org/jcp/copyright.jsp

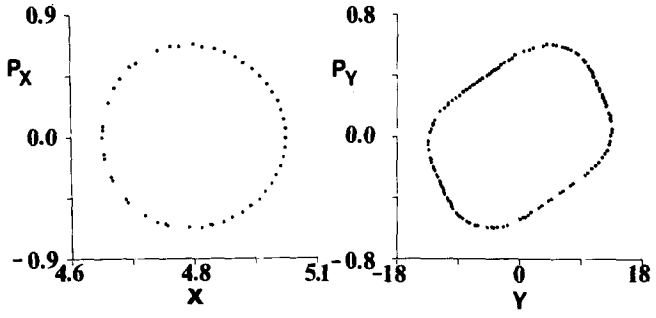

FIG. 3. A typical quasiperiodic trajectory for LiCN with energy 510 cm^{-1} which is below the isomerization barrier. (a) Poincaré surface of section for the stretching mode, (b) Poincaré surface of section for bending, and (c) the projection of the trajectory on the coordinate plane; labels as in Fig. 2.

Calculations were performed using program ATOMDIAT.[48] Optimized parameters for the Morse oscillator-like functions were found to be: $R_e = 4.18a_0$, $D_e = 14\,000$ cm^{-1}, $\omega_e = 417$ cm^{-1}. Table I demonstrates the convergence of the lowest 80 vibrational states with basis set size. All further LiCN calculations presented here used the 855 dimensional problem basis given by $n = 19$, $l = 44$. This basis converges the lowest 70 states to within 1 cm^{-1}, and mostly to within 0.1 cm^{-1}.

Analysis of the lowest 80 vibrational states of LiCN reveals a complicated picture. States corresponding to five different types can be observed.

A. Regular states localized about LiNC

The lowest 18 excited states are localized about the LiNC minimum and can easily be assigned according to their nodal structure (see Fig. 6). Above these are several states for which only approximate assignments are possible because of deformities in the nodal structure. Below the 80th excited state there are also a further eight regular states for which exact assignments can be made.

B. Irregular states localized about LiNC

Above the 18th excited state there are an increasing number of localized states which cannot easily be assigned (see Fig. 7). These range from states where distortion of the nodal structure makes an approximate assignment possible, to states for which no assignment can be made.

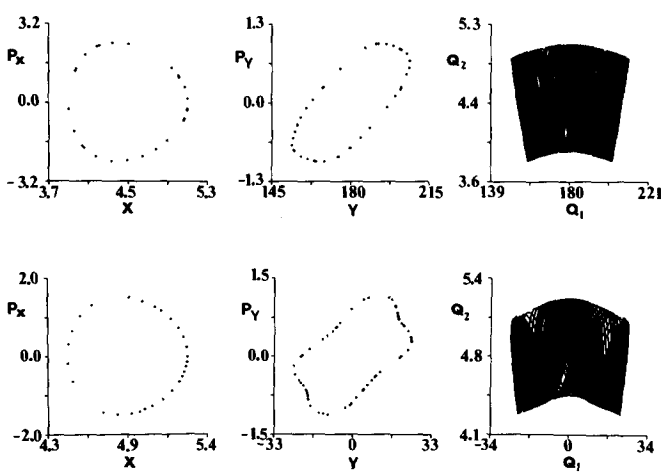

FIG. 4. Quasiperiodic trajectories above the isomerization barrier. Upper: LiNC at $E = 4460$ cm^{-1} lower: LiCN at $E = 2219$ cm^{-1}. (a), (b), and (c) as in Fig. 3.

C. Regular states localized about LiCN

The 30th excited state can be assigned as the LiCN ground state. Above this a further six states are localized about the LiCN local minimum. All these states can at least be approximately assigned according to their nodal structure (see Fig. 8). Some of these states are above the barrier to isomerization.

D. Irregular delocalized states

The 60th excited state and an increasing proportion of the higher states have significant amplitude on both sides of the potential barrier. Most of these states, including that shown in Fig. 9, have highly irregular nodal structures. When the radial zero point energy is allowed for, the 60th excited state and several other delocalized states lie below the barrier of 3377 cm^{-1} (from LiNC) between the two minima and thus display tunneling.

E. Free rotor or "polytopic" states

In 1973 Clementi *et al.*[49] predicted that LiCN should become polytopic (free rotor-like) above the barrier to isomerization. However, Brocks and Tennyson failed to observe any regular delocalized states.[37] Figure 10 shows

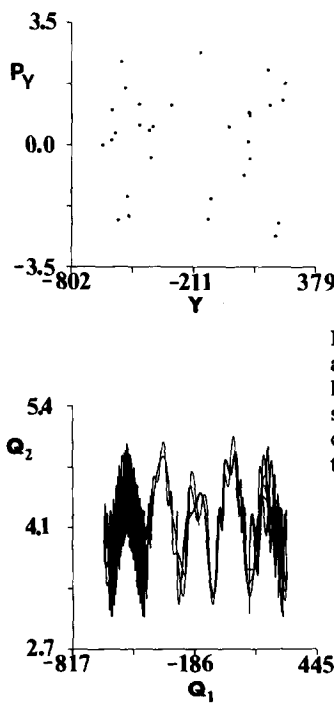

FIG. 5. A typical chaotic trajectory above the barrier to isomerization. Energy = 4217 cm^{-1} (a) Poincaré surface of section for the bending coordinate and (b) the projection of the trajectory on the coordinate plane.

Downloaded 08 Dec 2008 to 194.177.215.121. Redistribution subject to AIP license or copyright; see http://jcp.aip.org/jcp/copyright.jsp

TABLE I. Convergence of the vibrational states of LiCN with basis set. All energies are given relative to the ground state at −53 172.256 cm^{-1} in all calculations.

		Excited state							
n^a	l^b	10	20	30	40	50	60	70	79
15	44	1245.30	1874.83	2286.81	2669.81	2957.84	3223.49	3474.83	3662.91
17	44	1245.30	1874.83	2286.80	2669.52	2955.98	3223.42	3474.81	3660.03
17	48	1245.30	1874.83	2286.80	2669.52	2955.98	3223.42	3474.80	3659.99
19	44	1245.30	1874.83	2286.79	2669.48	2954.94	3223.41	3474.81	3655.34

[a] Number of Morse oscillator-like functions in the R basis.
[b] Maximum l in the Legendre function basis for θ.

two states which could be designated regular free rotor states on the basis of their nodal structure. The states have 24 and 26 nodes in the θ coordinate. We found no other delocalized states which were not some complex mix of bending and stretching coordinates (see Fig. 9).

Next we analyze the effect on the vibrational energy levels of small perturbations of the potential. For this the same perturbation is used as was used for KCN in I[39]:

$$V'(R, \theta) = V(R, \theta) + \delta P_2(\cos\theta) V_2(R). \quad (5)$$

Figure 11 shows the effect on the levels below 3000 cm^{-1} of small changes in δ. At lower energies [Fig. 11(a)] this perturbation causes only isolated avoided crossings, at higher energies [Fig. 11(b)] these crossings occur with increasing frequency. Above 2000 cm^{-1} (and perhaps lower) these avoided crossings can no longer be considered isolated.

We note that in many cases the levels approach closely before being repelled, suggesting that there is only weak coupling between the levels. This is in contrast to KCN (see I) where the levels are strongly repelled.

Figure 12 plots second differences calculated using Pomphrey's formula[9]

$$\Delta_i = |[E_i(+0.01) - E_i(0)] - [E_i(0) - E_i(-0.01)]|, \quad (6)$$

where $E_i(\delta)$ is the energy of the ith state calculated with a perturbation δ.

Comparison of Fig. 12 with Fig. 11 shows that the four pairs of states with large Δ_i (at about 1395, 1547, 2246, and 2918 cm^{-1}) all correspond to avoided crossings whose point of closest approach is for $\delta \approx 0.0$. Figure 13 gives second differences calculated according to Eq. (6) for KCN. Again, the largest values of Δ_i correspond to states in resonance (at about 300, 724, and 890 cm^{-1}).

Figure 14 shows two nearest neighbor level spacing distributions for LiCN. These spectral distributions have been plotted for the lowest 29 states and the next 51 states, respectively. This partitioning is rather arbitrary. Figure 14(a) corresponds to a region which is composed of states which can be assigned (at least approximately) by their nodal distribution. A Poisson distribution is also

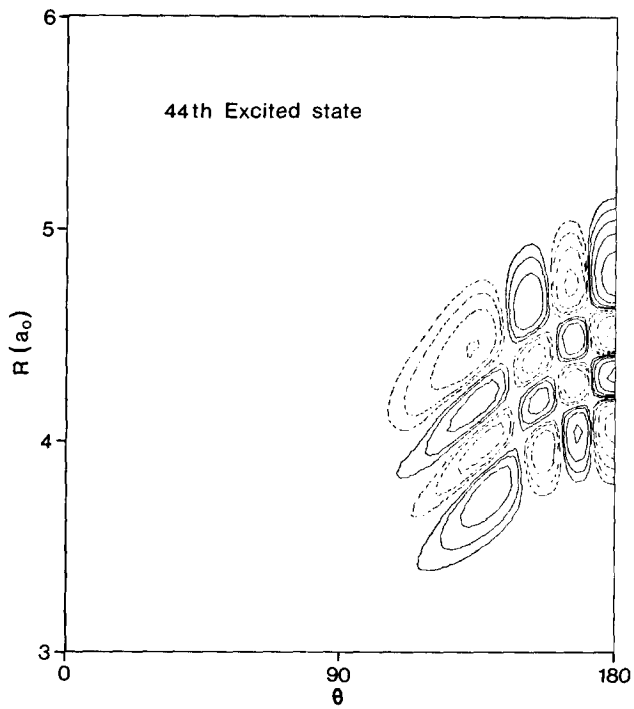

FIG. 6. Nodal structure of a typical regular LiNC state, ($v_{stretch}$, v_{bend}) = (3, 6). The contours link points where the wave function has 4%, 8%, 16%, 32%, and 64% of its maximum amplitude and dashed curves negative amplitude.

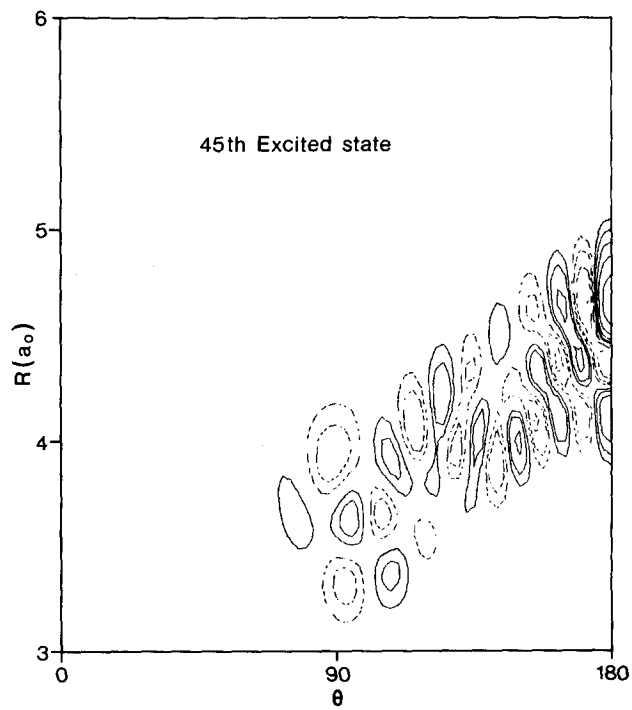

FIG. 7. A typical irregular LiNC state. Contours as in Fig. 6.

Downloaded 08 Dec 2008 to 194.177.215.121. Redistribution subject to AIP license or copyright; see http://jcp.aip.org/jcp/copyright.jsp

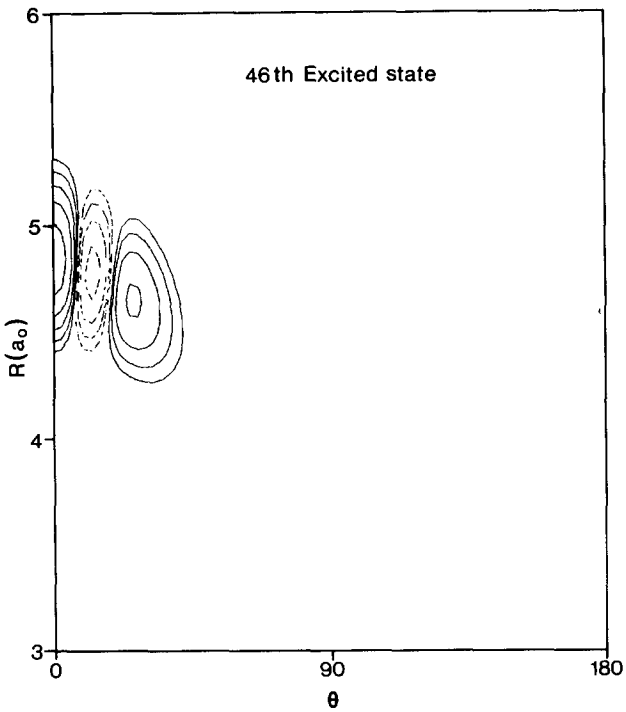

FIG. 8. A typical LiCN regular state ($v_{stretch}$, v_{bend}) = (0, 4). Contours as in Fig. 6.

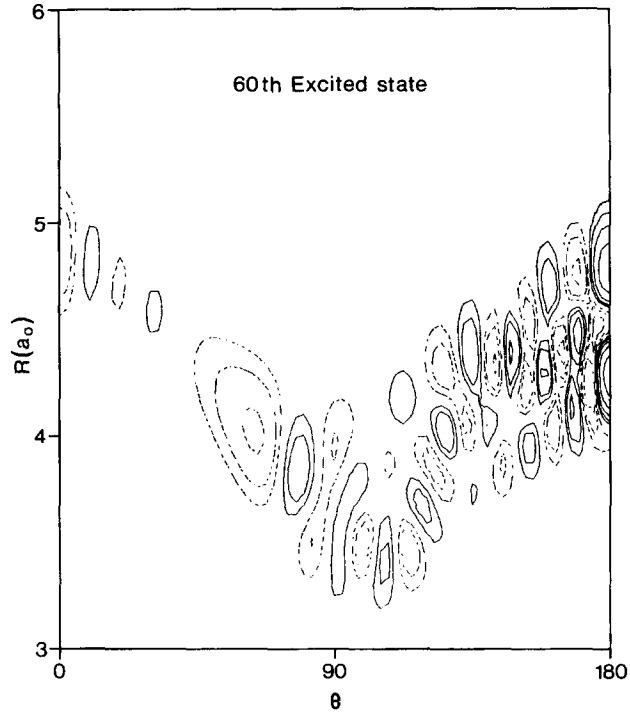

FIG. 9. An irregular delocalized state. Contours as in Fig. 6.

shown for comparison. For the higher levels, which cover a region where most of the states cannot readily be assigned, a Dyson–Wigner distribution is given [Fig. 14(b)]. Figure 15 shows the spacing of the KCN levels which also appear to approximately follow a Dyson–Wigner distribution.

IV. COMPARISON OF QUANTUM AND CLASSICAL RESULTS

The classical trajectory results presented in Sec. II show several interesting features. In the LiNC region of the potential chaos is found early, below the LiCN minimum, but localized quasiperiodic trajectories persist even above the LiNC/LiCN barrier. Starting from the LiCN minimum, quasiperiodic trajectories are again found above the barrier. All the delocalized trajectories we observed are chaotic.

LiNC and LiCN show a gradual reduction in the proportion of quasiperiodic trajectories above the critical energy. This is in accordance with KAM theory.[44] Conversely, KCN which has an even earlier onset of classical chaos, shows a sudden conversion to stochasticity.

How do these classical results compare with our quantum calculations? Analysis of nodal structures shows several of the features mentioned above. Above 1800 cm^{-1} localized LiNC vibrational states which cannot easily be assigned occur increasingly often. Some of these, including the lowest ones, are distorted regular states and can be labeled in an approximate fashion from their

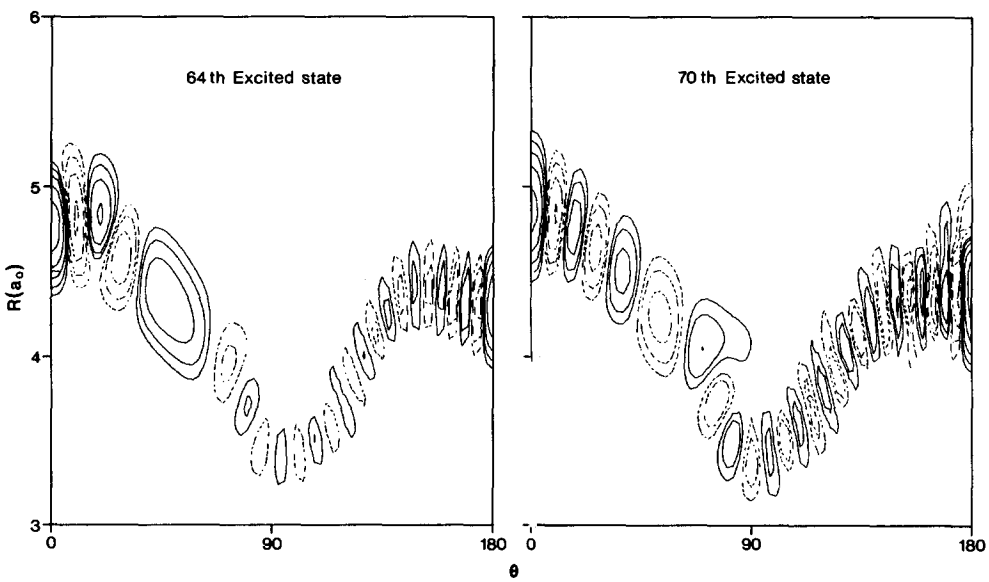

FIG. 10. Free rotor-like states. Contours as in Fig. 6.

Downloaded 08 Dec 2008 to 194.177.215.121. Redistribution subject to AIP license or copyright; see http://jcp.aip.org/jcp/copyright.jsp

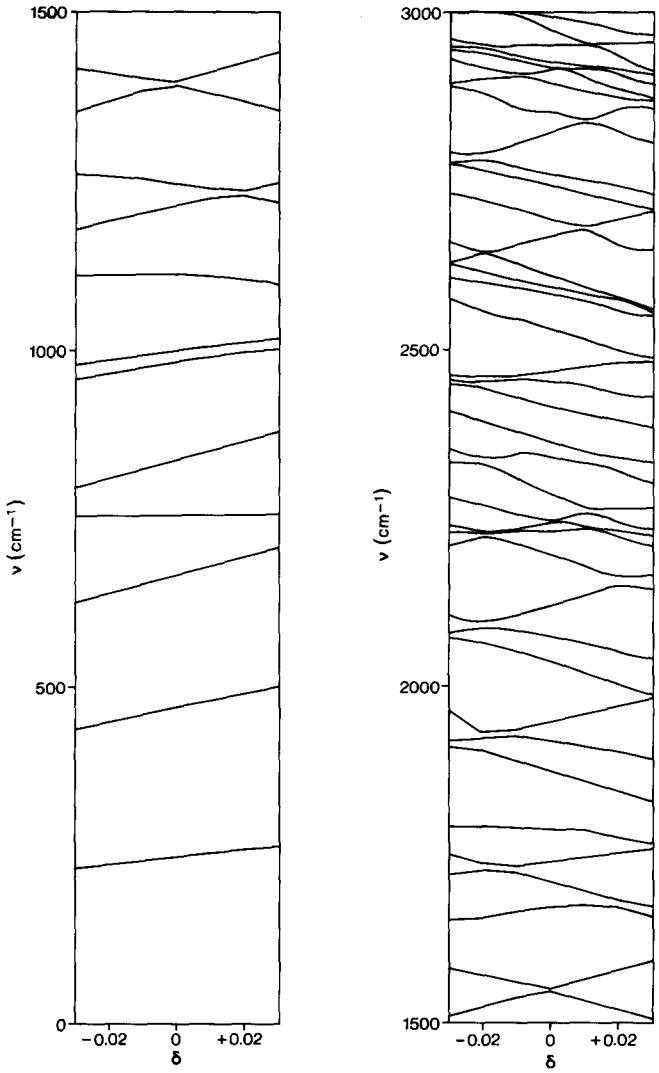

FIG. 11. Variation of vibrational frequency of LiCN with δ (see the text). All frequencies are plotted relative to the ground state.

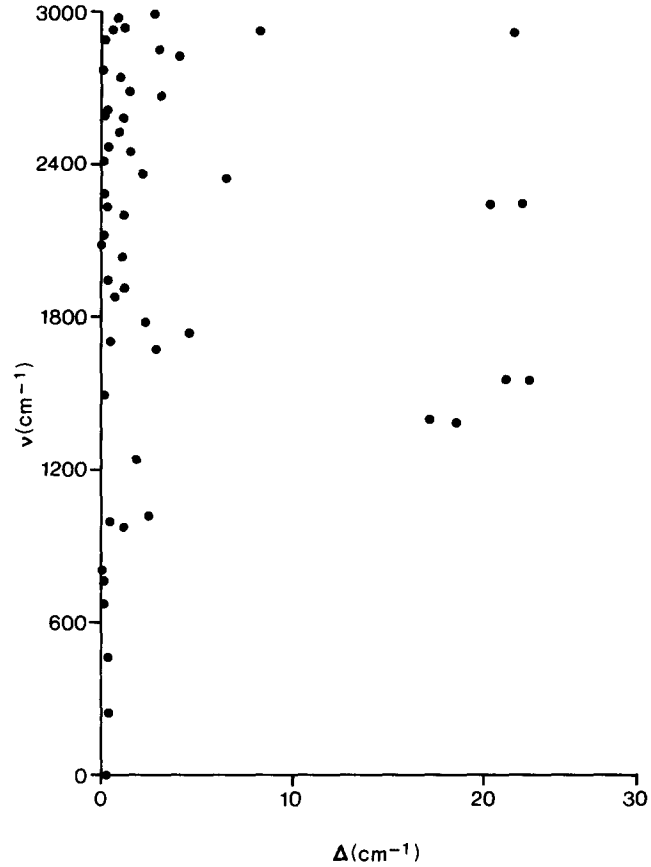

FIG. 12. Second differences for LiCN calculated using Eq. (6).

nodal structure; this was in fact done by Brocks and Tennyson.[37] Regular localized LiNC states persist through the energy range studied. Similarly regular LiCN states were found above the barrier. Most (all?) the delocalized quantum states have irregular nodal structures.

This gradual onset of irregularity in both LiCN and LiNC is again in contrast with the KCN results obtained in I. For KCN, no states above those which could be proved to be regular by the dominant coefficient criterion of Hose and Taylor,[8] could even approximately be assigned.

Analysis of the other criteria for quantum chaos gives further information. Perturbing the LiCN levels yields many overlapping avoided crossings in the region 2000+ cm^{-1} above the ground state. As in KCN, the exact transition point from isolated to overlapping avoided crossing is unclear.

In principle the second differences give a more quantitative measure of chaos. However, as was observed by Noid *et al.*[13] in their study of the Hénon–Heiles Hamiltonian, the largest second differences are due to near-resonant states undergoing avoided crossings. As avoided crossings are a feature of both regular and

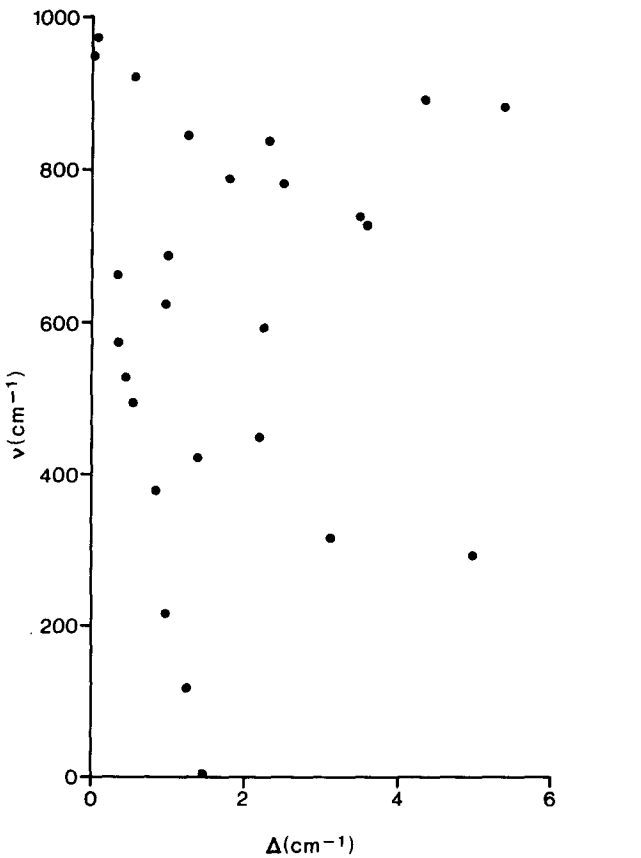

FIG. 13. KCN second differences.

Downloaded 08 Dec 2008 to 194.177.215.121. Redistribution subject to AIP license or copyright; see http://jcp.aip.org/jcp/copyright.jsp

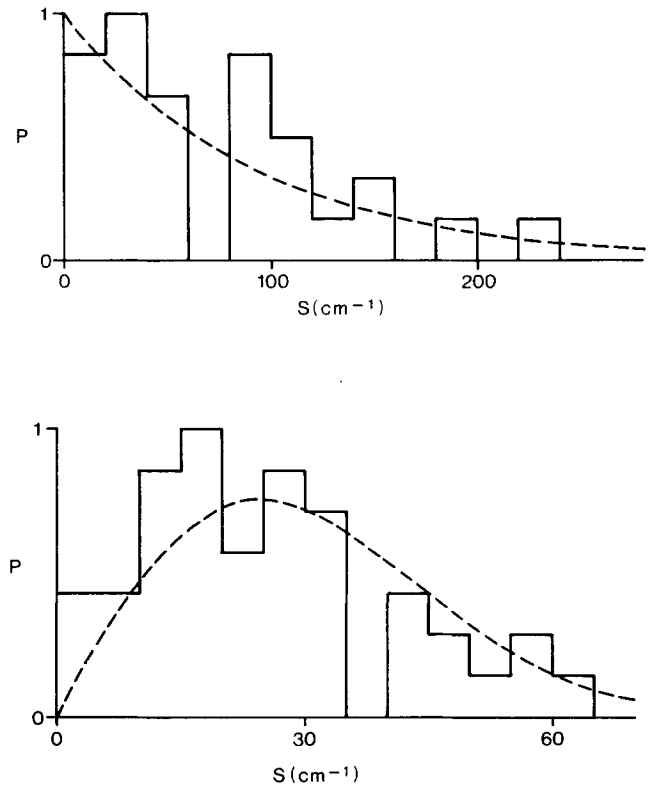

FIG. 14. Nearest neighbor level spacing histograms for LiCN. (a) the 29 lowest levels and (b) levels from 30 to 80.

irregular regions of the spectra these large second differences must be interpreted with caution.

Ignoring the large Δ_i due to the resonances, one can observe an increase in Δ_i with energy, especially in the LiCN results (see Fig. 12). This was again observed by Noid *et al.*[13] but appears contrary to the results of Pomphrey.[9] His analysis of the Hénon–Heiles problem showed a sharp increase in Δ_i in the chaotic region.

At best the spectral distributions, given here for LiCN (Fig. 14) and for KCN (Fig. 15), are only suggestive of the idealized distributions which we give for comparison. The comparatively small number of levels available in each case means that any statistical analysis is necessarily approximate.

The indicators of quantum chaos discussed above point to an early onset of chaos in LiCN. Although it is difficult to pinpoint where chaos first occurs there is good general agreement between the nodal structure, avoided crossings, and spectral distributions about which regions are regular and which chaotic. These regions of quantum regularity and chaos are in good agreement with those predicted classically. Indeed this qualitative correspondence also extends to nature of the chaotic regions, in particular to the strong and weak coupling displayed by KCN and LiCN, respectively.

Despite some sluggishness, chaos is found at low energies in both LiCN and KCN. This is in direct contrast to previous classical calculations on more conventional (less floppy) chemically bound systems such as O_3,[2] SO_2,[2] and HCN[30]. In none of these systems was chaos predicted at less than a third of the dissociation energy.

V. CRITERIA FOR QUANTUM CHAOS

In the light of our results on LiCN and KCN, it is interesting to consider the advantages and drawbacks of the five suggested indicators of quantum chaos.

Use of the nodal structure is potentially the most powerful of the suggested indicators. For example, it enabled us to establish good qualitative agreement between many features of our classical and quantum results in the last section. This is because nodal structure can be used to designate individual states (as opposed to regions) regular or chaotic. However this criterion must be used with caution because, as observed by De Leon *et al.*,[12] the occurrence of isolated Fermi resonances can cause regular states to appear irregular. This meant that the critical energy could not be precisely pinpointed in KCN. Conversely in a weakly coupled system such as LiCN, the loss of nodal regularity occurs only slowly again making the assignment of critical energy difficult.

The criterion of nodal structure is most easily used for two dimensional systems, such as those considered here. Making a similar analysis will clearly be much harder for polyatomic systems where the search for nodal hypersurfaces cannot easily be performed by graphical inspection.

Hose and Taylor's method of dominant coefficients[8] can in principle solve some of these problems as it is a numerical rather than topological measure. However, our experience has shown that basis functions which are suitable for representing the chaotic states of a system do not give dominant coefficients for the low-lying (quasi-periodic) levels. Although this problem might be overcome by transforming the one dimensional representations of the basis, we did not consider this worthwhile as this indicator yields no positive information about chaotic states.

The use of small perturbations of the potential gives two criteria for chaos which can be applied with equal ease to larger systems. Moreover, the use of avoided crossings is analogous to the explanation of classical chaos as overlapping nonlinear resonances. The occurrence of isolated avoided crossings can also be used to pinpoint states with irregular nodal structures due to Fermi reso-

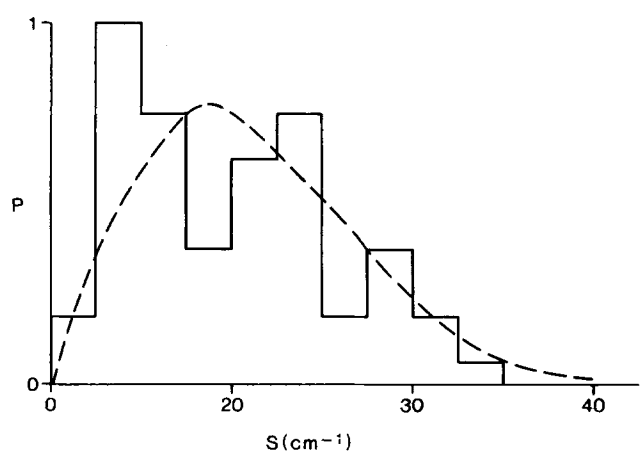

FIG. 15. Nearest neighbor level spacing histogram for KCN.

Downloaded 08 Dec 2008 to 194.177.215.121. Redistribution subject to AIP license or copyright; see http://jcp.aip.org/jcp/copyright.jsp

nance. This was done in I for KCN. However, we found it difficult to determine when crossings ceased to become isolated.

Another way of viewing this problem is: what constitutes a small or even a suitable perturbation? For model systems with one coupling parameter, such as the Hénon–Heiles problem, the choice of perturbation is unambiguous. For real systems, which have complicated potential functions there are many possible perturbations that can be applied; in our experience all perturbations do not have equal effect.

For example, Matsushita and Terasaka[11] recently analyzed the avoided crossings in a system of kinetically coupled Morse oscillators by varying the mass ratio of the component atoms. With this perturbation they successfully identified chaotic states in their system. Figure 16 shows the effect of changing the mass of K^+ on the vibrational levels of KCN. Although there are some avoided crossings, even in the region (400+ cm^{-1} above the ground state) where a considerably smaller perturbation of the potential [see Eq. (5)] caused many overlapping avoided crossings (see I), there is little evidence of any chaotic behavior with this perturbation of the kinetic energy operator. Similarly, even comparatively large perturbations of the whole potential:

$$V'(R, \theta) = (1 + \delta)V(R, \theta) \tag{7}$$

caused few crossings in this system.

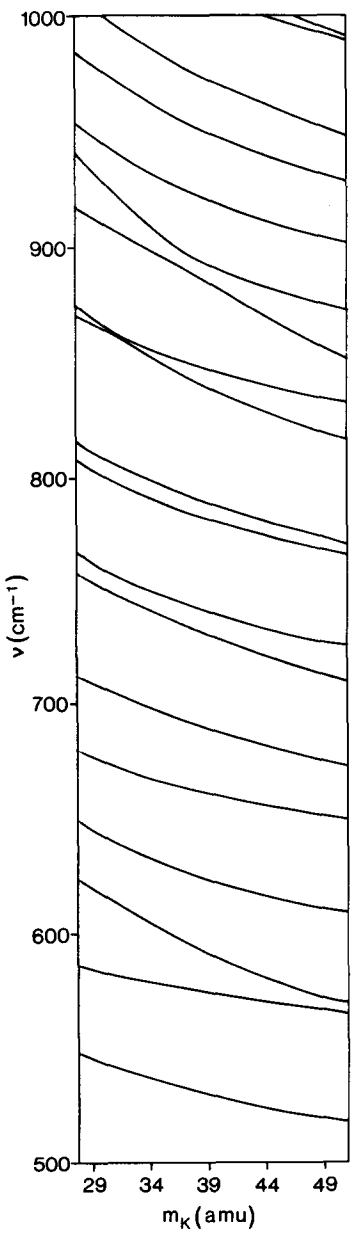

FIG. 16. Variation of KCN vibrational frequencies with the mass of potassium. All frequencies are plotted relative to the ground state. There are no avoided crossings below 500 cm^{-1}.

This sensitivity to perturbation emphasizes the need to perturb the coupling term in the Hamiltonian which is responsible for the onset of chaos. In our case this is the anisotropic part of the potential; in Matsushita and Terasaka's calculation it is the kinetic energy operator. For a complex real calculation, however, the nature of the coupling may not be immediately apparent.

The use of second differences rather than avoided crossings is attractive because it is a numerical rather than graphical indicator. However, in agreement with Noid *et al.*,[13] we found that this test highlighted resonant rather than necessarily chaotic states.

The use of spectral distributions did not prove particularly useful for either LiCN or KCN. This is because the low density of states in these small molecules means that insufficient levels are available for accurate statistical analysis. However, in polyatomic molecules this should no longer be the case and the experimental applicability of this indicator[26,27] gives it an advantage over all the others we consider.

VI. CONCLUSION

The vibrational motions of the floppy LiCN and KCN molecules have been studied both classically and quantum mechanically. All the criteria analyzed point to an early onset of quantum chaos in both these systems. Two criteria nodal structure and overlapping avoided crossings gave useful information about these systems; a third, spectral distributions, can be expected to be of greater use for polyatomic systems. Our experience suggests that it is necessary to study more than one criterion to obtain maximal information about the system. Conversely, we found neither second differences nor Hose and Taylor's "Quantum KAM-like theory"[8] helpful in interpreting our results.

Good qualitative agreement between quantum and classical mechanics is obtained for both LiCN and KCN. Although there is some quantum sluggishness, the early onset (very early in KCN) is predicted in both mechanics. Furthermore, in both the markedly different behavior between strongly coupled KCN and weakly coupled LiCN is apparent. Indeed both our quantum and classical calculations find that regular motion, localized about LiNC and LiCN persists well into the chaotic region and above the barrier between the two LiCN structures. The systematics behind this regular motion and its consequences for the spectroscopy of small molecules will be the subject of a forthcoming article.[50]

Downloaded 08 Dec 2008 to 194.177.215.121. Redistribution subject to AIP license or copyright; see http://jcp.aip.org/jcp/copyright.jsp

Our results demonstrate the association between the early onset of chaos and floppiness. The nature of chaos is such that our calculations can have little directly predictive worth in the chaotic region as any improvement to the potential can be expected to alter dramatically the chaotic vibrational levels. However, we can suggest that experimentalists interested in investigating vibrational chaos should look at floppy systems such as LiCN and KCN.

ACKNOWLEDGEMENT

One of us (S.C.F.) wishes to thank the Royal Society and the British Council for financial support and Daresbury Laboratory for hospitality while some of this work was completed.

[1] D. W. Noid, M. L. Koszykowski, and R. A. Marcus, Ann. Rev. Phys. Chem. **32,** 267 (1981).
[2] S. C. Farantos and J. N. Murrell, Chem. Phys. **55,** 205 (1981).
[3] S. C. Farantos, Chem. Phys. Lett. **92,** 379 (1982).
[4] S. C. Farantos, J. Phys. Chem. **87,** 5061 (1983).
[5] M. D. Feit and J. A. Fleck Jr., J. Chem. Phys. **80,** 2578 (1984).
[6] A. R. Edmonds, R. A. Pullen, and I. C. Percival, Chem. Phys. Lett. **91,** 273 (1982).
[7] R. M. Stratt, N. C. Handy, and W. H. Miller, J. Chem. Phys. **71,** 3311 (1979).
[8] G. Hose and H. S. Taylor, J. Chem. Phys. **76,** 5356 (1982); **78,** 5845 (1983); S. Mukamel, *ibid.* **78,** 5843 (1983); G. Hose and H. S. Taylor, Phys. Rev. Lett. **51,** 947 (1983); G. Hose, H. S. Taylor, and A. Tip, J. Phys. A **17,** 1203 (1984).
[9] N. Pomphrey, J. Phys. B **7,** 1909 (1974).
[10] D. W. Noid, M. L. Koszykowski, and R. A. Marcus, Chem. Phys. Lett. **73,** 269 (1980); J. Chem. Phys. **78,** 4018 (1983).
[11] T. Matsushita and T. Terasaka, Chem. Phys. Lett. **105,** 511 (1983).
[12] N. De Leon, M. J. Davis, and E. J. Heller, J. Chem. Phys. **80,** 794 (1984).
[13] D. W. Noid, M. L. Koszykowski, M. Tabor, and R. A. Marcus, J. Chem. Phys. **72,** 6169 (1980).
[14] Y. Weissman and J. Jortner, Chem. Phys. Lett. **78,** 224 (1981).
[15] R. Ramaswamy and R. A. Marcus, J. Chem. Phys. **74,** 1385 (1981).
[16] M. V. Berry and M. Tabor, Proc. R. Soc. London Ser. A **356,** 375 (1977).
[17] J. S. Hutchinson and R. E. Wyatt, Phys. Rev. A **23,** 1567 (1981).
[18] M. L. Koszykowski, D. W. Noid, M. Tabor, and R. A. Marcus, J. Chem. Phys. **74,** 2530 (1983).
[19] S. Abe and S. Mukamel, J. Chem. Phys. **79,** 5457 (1983).
[20] M. Shapiro, R. D. Taylor, and P. Brumer, Chem. Phys. Lett. **106,** 325 (1984).
[21] W. P. Reinhardt, in *The Mathematical Analysis of Physical Systems,* Edited by R. Mickens (Van Nostrand, New York, 1984).
[22] The results of Feit and Fleck (Ref. 5) would appear to contradict this statement. However, the quasiperiodic trajectories they present are at significantly lower energy than their chaotic quantum states. This appears to invalidate any correspondence.
[23] R. A. Marcus, J. Chem. Soc. Faraday Discuss **75,** 103 (1983).
[24] E. Haller, H. Köppel, and L. S. Cederbaum, Chem. Phys. Lett. **101,** 215 (1983).
[25] I. C. Percival, J. Phys. B **6,** L229 (1973); Adv. Chem. Phys. **36,** 1 (1977).
[26] H. S. Camarda and P. D. Georgopulos, Phys. Rev. Lett. **50,** 492 (1983).
[27] E. Abramson, R. W. Field, D. Imre, K. K. Innes, and J. L. Kinsey, J. Chem. Phys. **80,** 2298 (1984).
[28] M. V. Berry, in *Chaotic Behaviour in Deterministic Systems,* edited by G. Iooss, R. H. G. Helleman, and R. Stora (North-Holland, Amsterdam, 1984).
[29] E. J. Heller, J. Chem. Phys. **72,** 1337 (1980).
[30] K. K. Lehmann, G. J. Scherer, and W. Klemperer, J. Chem. Phys. **77,** 2853 (1982); **78,** 608 (1983); D. Farrelly and W. P. Reinhardt, *ibid.* **78,** 606 (1983).
[31] T. Torring, J. P. Bekooy, W. L. Meerts, J. Hoeft, E. Tiemann, and A. Dymanus, J. Chem. Phys. **73,** 4875 (1980).
[32] J. J. van Vaals, W. L. Meerts, and A. Dymanus, Chem. Phys. **86,** 147 (1984); J. Mol. Spectrosc. (in press).
[33] J. J. van Vaals, W. L. Meerts, and A. Dymanus, Chem. Phys. (in press).
[34] J. Tennyson and B. T. Sutcliffe, Mol. Phys. **46,** 97 (1982).
[35] J. Tennyson and A. van der Avoird, J. Chem. Phys. **76,** 5710 (1982).
[36] J. Tennyson and B. T. Sutcliffe, J. Chem. Phys. **77,** 4061 (1982).
[37] G. Brocks and J. Tennyson, J. Mol. Spectrosc. **99,** 263 (1983).
[38] G. Brocks, J. Tennyson, and A. van der Avoird, J. Chem. Phys. **80,** 3223 (1984).
[39] J. Tennyson and S. C. Farantos, Chem. Phys. Lett. **109,** 160 (1984).
[40] P. E. S. Wormer and J. Tennyson, J. Chem. Phys. **75,** 1245 (1981).
[41] R. Essers, J. Tennyson, and P. E. S. Wormer, Chem. Phys. Lett. **89,** 223 (1982).
[42] Z. K. Ismail, R. H. Hauge, and J. L. Margrave, J. Chem. Phys. **57,** 5137 (1972).
[43] D. L. Bunker and W. L. Hase, J. Chem. Phys. **59,** 4621 (1973).
[44] V. I. Arnold and Avez, *Ergodic Problems in Classical Mechanics* (Benjamin, New York, 1968).
[45] Ya. G. Sinai, *Introduction to Ergodic Theory* (Princeton University, Princeton, 1976).
[46] N. S. Krylov, *Works on the Foundation of Statistical Physics* (Princeton University, Princeton, 1979).
[47] K. D. Hänsel, Chem. Phys. **33,** 35 (1978); N. De Leon and B. J. Bern, Chem. Phys. Lett. **93,** 162 (1982).
[48] J. Tennyson, Comput. Phys. Commun. **29,** 307 (1983).
[49] E. Clementi, H. Kistenmacher, and H. Popkie, J. Chem. Phys. **58,** 2460 (1973).
[50] J. Tennyson and S. C. Farantos, Chem. Phys. (in press).

Downloaded 08 Dec 2008 to 194.177.215.121. Redistribution subject to AIP license or copyright; see http://jcp.aip.org/jcp/copyright.jsp